Received: 26 April 2021 | Revised: 5 August 2021 | Accepted: 9 August 2021

DOI: 10.1002/mrm.28988

RESEARCH ARTICLE

Magnetic Resonance in Medicine

Optimization of pseudo-continuous arterial spin labeling at 7T with parallel transmission B1 shimming

Kai Wang[1] | **Samantha J. Ma**[1,2] | **Xingfeng Shao**[1] | **Chenyang Zhao**[1] | **Qinyang Shou**[1] | **Lirong Yan**[1,3] | **Danny J. J. Wang**[1,3]

[1]Laboratory of FMRI Technology, USC Mark & Mary Stevens Neuroimaging and Informatics Institute, Keck School of Medicine, University of Southern California, Los Angeles, California, USA

[2]Siemens Medical Solutions USA, Los Angeles, California, USA

[3]Department of Neurology, Keck School of Medicine, University of Southern California, Los Angeles, California, USA

Correspondence
Danny J. J. Wang, Laboratory of FMRI Technology, USC Mark & Mary Stevens Neuroimaging and Informatics Institute, Keck School of Medicine, University of Southern California, Los Angeles, CA, USA.
Email: jwang71@gmail.com

Funding information
National Institutes of Health; Grand/Award Nos. UH3-NS100614, S10-OD025312, R01-NS114382, R01-EB028297, R01-EB032169 and R01-NS118019

Purpose: To optimize pseudo-continuous arterial spin labeling (pCASL) for 7 T, and to further improve the labeling efficiency with parallel RF transmission transmit B_1 (B_1^+) shimming.

Methods: pCASL parameters were optimized based on B_1^+/B_0 field distributions at 7 T with simulation. To increase labeling efficiency, the B_1^+ amplitude at inflowing arteries was increased with parallel RF transmission B_1^+ shimming. The "indv-shim" with shimming weights calculated for each individual subject, and the "univ-shim" with universal weights calculated on a group of 12 subjects, were compared with circular polarized (CP) shim. The optimized pCASL sequences with three B_1^+ shimming modes (indv-shim, univ-shim, and CP-shim) were evaluated in 6 subjects who underwent two repeated scans 24 hours apart, along with a pulsed ASL sequence. Quantitative metrics including mean B_1^+ amplitude, perfusion, and intraclass correlation coefficient were calculated. The optimized 7T pCASL was compared with standard 3T pCASL on 5 subjects, using spatial SNR and temporal SNR.

Results: The optimal pCASL parameter set (RF duration/gap = 300/250 us, $G_{ave} = 0.6\,\mathrm{mT/m}$, $gRatio = 10$) achieved robust perfusion measurement in the presence of B_1^+/B_0 inhomogeneities. Both indv-shim and univ-shim significantly increased B_1^+ amplitude compared with CP-shim in simulation and in vivo experiment ($P < .01$). Compared with CP-shim, perfusion signal was increased by 9.5% with indv-shim ($P < .05$) and by 5.3% with univ-shim ($P = .35$). All three pCASL sequences achieved fair to good repeatability (intraclass correlation coefficient ≥ 0.5). Compared with 3T pCASL, the optimized 7T pCASL achieved 78.3% higher spatial SNR and 200% higher temporal SNR.

Conclusion: The optimized pCASL achieved robust perfusion imaging at 7 T, while both indv-shim and univ-shim further increased labeling efficiency.

KEYWORDS
arterial spin labeling, B_1^+ shimming, parallel RF transmission, perfusion, ultrahigh field, universal pulse

1 | INTRODUCTION

Arterial spin labeling (ASL) techniques have recently been implemented at ultrahigh field (UHF) to take advantage of the dual benefits for SNR improvement: the increased intrinsic SNR with a superlinear relationship with static magnetic field (~$B_0^{1.65}$) and the prolonged tracer half-life (arterial blood T_1).[2] However, there remain considerable obstacles to reliably implement ASL sequences at UHF. For pulsed ASL (PASL), the transmit B_1 field (B_1^+) inhomogeneity and the B_0 offset make it challenging to achieve efficient labeling and clean background tissue subtraction, even with adiabatic inversion pulses. For pseudo-continuous ASL (pCASL), the B_1^+ and B_0 field inhomogeneities at the labeling plane undermine the flow-driven adiabatic inversion condition, resulting in low labeling efficiency.[3-5]

A number of studies have been performed to address the challenges for implementing ASL at UHF. For PASL, several adiabatic inversion pulses have been proposed,[6-8] optimized, and evaluated[9-11] for flow-sensitive alternating inversion recovery; for pCASL, the labeling plane was raised from the neck to the bottom of the cerebrum to take advantage of the higher B_1^+ amplitude.[12] Alternatively, dielectric pads were used to increase B_1^+ amplitude and homogeneity,[13] and a prescan was used to correct for off-resonance effects at the labeling plane.[14] However, few studies have been performed to optimize the parameters for pCASL based on the specific distributions of B_1^+ and B_0 field at UHF.

Parallel RF transmission (pTx) provides additional degrees of freedom that allow full spatial and temporal control of the B_1^+ field. With a transmit coil array that consists of several elements with spatially distinct B_1^+ field pattern and channel-specific RF pulse waveform, the extra degrees of freedom can be exploited to overcome the effect of B_1^+ inhomogeneity for implementing ASL at UHF. Recently, Tong et al[15] used pTx B_1^+ shimming to minimize the difference between the actual flip angle (FA) and the target value, and variable-rate selective excitation (VERSE) was further used to decrease the specific absorption rate (SAR) of RF power. However, the pCASL labeling parameters were adopted directly from 3 T, which may not be suited for 7T scans, and the shimming weight had to be calculated for each subject, which prolonged the total scan time and presented a challenge for clinical translation. Gras et al[16] developed the "universal pulse" to design a dynamic pTx pulse that is optimized for a group of subjects and therefore is calibration-free for individual subjects. However, the optimal design of "universal pulse" for pCASL is challenging and has never been attempted, given the flowing spins that confound the precise control of the excitation k-space as well as the complex geometry of inflowing arteries.

The overarching goal of this study was to develop robust pCASL perfusion imaging at 7 T with pTx shimming technologies. We first optimized pCASL labeling parameters based on the B_1^+ and B_0 distributions at 7 T[11]; then the optimized pCASL was implemented with pTx B_1^+ shimming using individually optimized weights ("indv-shim") and a "universal weight" optimized on a separate cohort ("univ-shim"), which does not require any calibration steps. We further compared the performance of the optimized 7T pCASL with a standard 3T pCASL. We demonstrated that the optimized pCASL was able to obtain reliable perfusion maps at 7 T with increased SNR compared with 3T pCASL and that both indv-shim and univ-shim further improved the labeling efficiency.

2 | METHODS

2.1 | Simulation of pCASL labeling parameter optimization

Based on the principle of pCASL,[5] a pCASL labeling block can be determined by the following parameters: the RF FA, RF duration, RF gap, mean gradient G_{ave}, and gradient amplitude during each RF pulse G_{max}, as shown in Supporting Information Figure S1. The value of G_{max} can be expressed as $G_{ave} \cdot gRatio$. A commonly used set of pCASL parameters at 3 T include RF FA = 25°, RF duration = 500 us, RF gap = 420 us, G_{ave} = 0.6 mT/m, and $gRatio$ = 10,[5,17] noted as "labeling 0."

To optimize pCASL at 7 T, numerical simulation was performed to estimate the labeling efficiency (LE) for a wide range of pCASL parameters: Hanning-shaped RF pulse, RF duration = [300:100:1000] us, G_{ave} = [0.1:0.1:1.2] mT/m, and $gRatio$ = [5:1:15]. The RF gap was determined such that the ratio between RF gap and RF duration was the same as labeling 0 for the duty cycle of the RF power amplifier for playing out the pCASL pulses to remain constant (54.35%), and the RF FA was determined to maintain the same time-averaged SAR. The flow velocity was assumed to be 40 cm/s.[18] Assuming blood T_1 = 2100 ms[2] and T_2 = 60 ms,[19] Bloch equation simulation[20] was performed with a time interval of 10 us. The LE was defined as the subtraction of the inversion efficiency between label and control (180° phase increment between adjacent RF pulses) conditions.

The balanced pCASL scheme was used to avoid the effects of eddy current.[3]

The B_1^+ and B_0 inhomogeneities were incorporated in the optimization by considering B_1^+ amplitude of [20:10:120]% of reference B_1^+, and B_0 offset with a range of [–200:20:200] Hz. The weighting for each B_1^+/B_0 condition was estimated from 44 inflowing arteries (left and right internal carotid arteries and vertebral arteries) of 11 subjects in a previously published cohort (Supporting Information Section 2) with the following process: First, for each subject, time-of-flight (TOF) images were acquired to obtain angiography, the labeling plane was placed at the C1 segment (Bouthillier classification) of the internal carotid arteries (Figure 1A), and a B_1^+ (Figure 1B) and B_0 map (Figure 1C) were acquired at the labeling plane with turbo fast-low-angle-shot (TFL) and gradient-echo sequences, respectively. Second, the regions of interest (ROIs) of the four inflowing arteries were manually drawn on the TOF image. Third, the ROIs were resampled to match the voxel size of B_1^+ and B_0 maps, respectively, and the mean B_1^+ amplitude and B_0 offset were calculated for each artery. The histograms of the relative B_1^+ amplitude scaling (mean ± SD: 0.71 ± 0.11) and the B_0 offset (–78.8 ± 49.7 Hz) are shown in Figure 1D,E, respectively, and the LE of each set of pCASL labeling parameters was calculated as the weighted average of the LE of all B_1^+/B_0 conditions, with the relative frequency of each B_1^+/B_0 condition as the weighting. Therefore, the optimal set of pCASL parameters was chosen as the one with the highest weighted average of LE, noted as "labeling 1."

2.2 | Pseudo-continuous ASL implementation and optimization

A pCASL sequence with 2D TFL readout[12] was implemented with the following parameters: FOV = 210 × 192.5 mm, matrix size = 96 × 60, nine slices with 5-mm thickness and 2.5-mm interslice gap, slice acquisition duration = 150 ms, partial Fourier = 6/8, sequential k-space ordering, TR = 6000 ms, TE = 1.38 ms, FA = 8°, labeling duration = 1000 ms, postlabeling delay = 1500 ms, and 40 measurements including two M_0 scans and 19 label/control pairs for 4:02 minutes.

Four sets of pCASL parameters were evaluated: (1) the benchmark parameters (labeling 0); (2) the parameters optimized by simulation (labeling 1); (3) RF (FA, duration, and RF gap) of labeling 1 and gradient (G_{ave} and $gRatio$) of labeling 0 ("labeling 2"); and (4) same as labeling 2, except that the RF gap was reduced so that the gradient slew rate reached hardware limit ("labeling 3"). Labeling 2 was implemented to ameliorate the possible aliasing problem (see sections 2 and 3), whereas labeling 3 was implemented to further minimize the RF gap on top of labeling 2.

Four subjects were recruited (2 males, age = 28.8 ± 8.9 years, weight = 57.8 ± 11.2 kg, height = 170.3 ± 9.0 cm) to evaluate the performance of the four parameter sets. This study was approved by the institutional review board of the University of Southern California, and written informed consent was obtained before the experiments from each subject. In vivo experiments were performed on a 7T MRI MAGNETOM Terra (Siemens Healthcare, Erlangen,

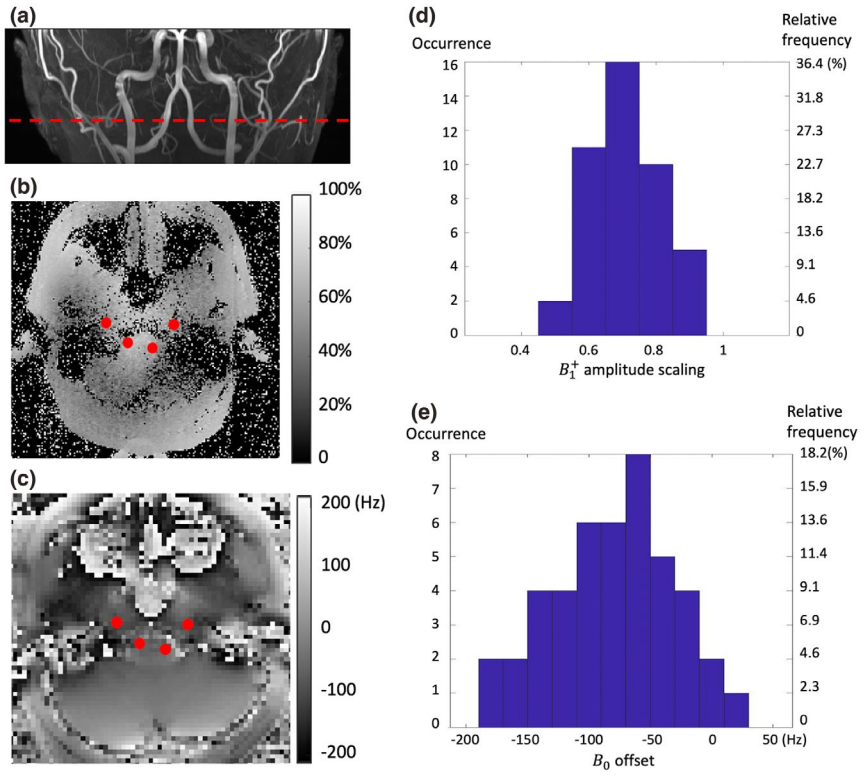

FIGURE 1 A, The red dashed line shows the labeling plane on top of the maximum intensity projection on the coronal plane of time of flight. B, The B_1^+ amplitude map, normalized by the designed value. C, The B_0 map. D,E, Histogram for the distribution of B_1^+ scaling (0.71 ± 0.11) and B_0 offset (78.8 ± 49.7 Hz), measured at the total of 44 inflowing arteries of the 11 subjects (left and right internal carotid arteries and vertebral arteries in each subject)

Germany) with an 8-transmit/32-receive head coil (Nova Medical, Wilmington, MA).

To calculate perfusion maps for the pCASL sequences, images were corrected for rigid head motion using *SPM12* (Wellcome Trust Centre for Neuroimaging, University College London); then, pairwise subtraction of label and control images was performed, followed by averaging across measurements. The perfusion maps were then normalized by the M_0 image resulting in fractional perfusion maps. The four sets of labeling parameters were evaluated based on two criteria: (1) perfusion images without distortion or contamination by the side lobes of labeling pulses, and (2) LE indicated by fractional perfusion signal intensity. The pCASL parameter set, which yielded the highest fractional perfusion signal without distortion or contamination of perfusion images, would be considered as the optimal parameter set for 7T pCASL.

2.3 | Parallel transmit B_1^+ shimming

2.3.1 | Optimization of indv-shim

To mitigate the B_1^+ drop at the labeling plane (typically at the bottom edge of the cerebellum), B_1^+ shimming was used to increase the B_1^+ amplitude at the inflowing arteries for each individual subject: The channel-specific B_1^+ maps were acquired at the labeling plane, and the voxel-wise B_1^+ values within the four ROIs of the inflowing arteries (Figure 1B) were fed into the B_1^+ shimming optimization algorithm.

A cost function was defined for B_1^+ shimming optimization, which consists of an efficiency term and an asymmetry term. The efficiency term penalized low B_1^+ amplitude by taking the form of $Eff = -\left\|\boldsymbol{B}_{chn}\cdot\boldsymbol{u}\right\|^2$, where $\boldsymbol{B}_{chn}$ is the channel-specific B_1^+ of the voxels within the ROIs and $\boldsymbol{u}$ is the complex weight for each channel. The asymmetry term was designed specifically to penalize the inter-hemispheric B_1^+ difference of the left and right arteries, which would cause imbalanced perfusion signal of the left and right hemispheres. It was defined as the square of the amplitude of the difference between the B_1^+ amplitude of the left and right ROIs: $Asym = \left\|\left|\boldsymbol{B}_{chn,left}\cdot\boldsymbol{u}\right| - \left|\boldsymbol{B}_{chn,right}\cdot\boldsymbol{u}\right|\right\|^2$. Anterior–posterior asymmetry was not included, as it would lead to decreased B_1^+ amplitude at the internal carotid arteries. The cost function was then defined as a weighted sum of the two terms, as follows:

$$\begin{aligned} cost &= Eff + w\cdot Asym \\ &= -\left\|\boldsymbol{B}_{chn}\cdot\boldsymbol{u}\right\|^2 + w\cdot\left\|\left|\boldsymbol{B}_{chn,left}\cdot\boldsymbol{u}\right| - \left|\boldsymbol{B}_{chn,right}\cdot\boldsymbol{u}\right|\right\|^2 \end{aligned} \quad (1)$$

where w is the weighting for the asymmetry term. Therefore, $\boldsymbol{u}$ was optimized by minimizing the cost function using the "fmincon" solver of *MATLAB* (The MathWorks, Natick, MA), during which only the phases of $\boldsymbol{u}$ were updated. A flowchart of the optimization process is shown in Supporting Information Figure S2.

The True-Form mode implemented by the vendor,[21] which uses the same amplitude and 45° phase increment for each adjacent transmit channel to mimic the single transmit circularly polarized (CP) coil, served as the benchmark, noted as "CP-shim." Similar to the definition of the efficiency term and asymmetry term in the cost function, two metrics were defined to evaluate the proper asymmetry term weighting w: $r\mathrm{MeanB1}$, which is the mean B_1^+ amplitude within ROIs, and $r\mathrm{Asym}$, which is the mean absolute value of the left and right B_1^+ amplitude difference divided by $r\mathrm{MeanB1}$. These two metrics were calculated over $w \in [0, 50]$, and the ratio of the shimming mode and the CP-shim was calculated for both $r\mathrm{MeanB1}$ and $r\mathrm{Asym}$. The optimal w was manually selected based on the rMeanB1 ratio-w and rAsym ratio-w curves: Ans rMeanB1 ratio > 1, which means increased B_1^+ amplitude compared with CP-shim, and a rAsym ratio < 1, which means decreased asymmetry compared with CP-shim, were required. The weighting selection process was performed on 2 representative subjects from a previously acquired cohort (n = 12; see Supporting Information Section 4), and the optimal w was used for all subjects of the in vivo experiments (section 2.4). The B_1^+ shimming weight calculated per subject is noted as "individual weight," and the shimming method is noted as "indv-shim."

2.3.2 | Universal weight

Considering the extra time and manual operation needed to calculate the individual weight, a "universal weight" was developed without the need for adjustments for individual subjects during the scan. The development and evaluation of universal weight were performed on a previously acquired subject cohort (n = 12; see Supporting Information Section 4). The optimization process was similar to that of indv-shim, except that the cost function was calculated with all 48 ROIs from 12 subjects. This shimming method is noted as "univ-shim."

Numerical simulation was used to evaluate the univ-shim with leave-one-out cross-validation: One universal weight was calculated with 11 subjects, and then evaluated on the remaining subject. Because the optimal asymmetry weighting w may be different from that of indv-shim, the weighting evaluation process was repeated by calculating the $r\mathrm{MeanB1}$ and $r\mathrm{Asym}$ metrics over $w \in [0, 50]$, averaged across 12 subjects. For comparison, the $r\mathrm{MeanB1}$ and $r\mathrm{Asym}$ metrics were also calculated with the B_1^+ shimming results of CP-shim and indv-shim. Once the method of univ-shim was verified, a final universal weight was calculated with all 12 subjects and applied in the in vivo experiments.

2.4 | In vivo experiment: robustness and repeatability

Six subjects were recruited (3 males, age = 25.8 ± 3.2 years, weight = 60.7 ± 12.1 kg, and height = 169.2 ± 11.8 cm) for this validation study. Each subject underwent two scans that were 24 hours apart to control for daily physiological fluctuation of brain perfusion.

The scan protocol for each visit is listed in Supporting Information Table S1, which included (1) a time-of-flight sequence for the localization of labeling plane and inflowing arteries; (2) a modified TFL sequence to acquire channel-specific B_1^+ map; (3) three pCASL sequences with labeling parameters optimized in sections 2.1 and 2.2 with CP-shim, indv-shim, and univ-shim, respectively; and (4) a pulsed ASL sequence optimized in a previous study[11] as a comparison for the pCASL sequences. The labeling plane position was the same for all pCASL sequences (Figure 1A). The FOV and B_0 shimming volume were kept the same for all ASL sequences.

The performance of B_1^+ shimming was evaluated by calculating the rMeanB1 and rAsym metrics for each subject of each B_1^+ shimming mode, respectively. The process of preprocessing and perfusion map calculation was the same as the pCASL parameter optimization study (section 2.2). The mean gray matter (GM) fractional perfusion signal (normalized by M_0) was calculated for each subject, each visit, and each ASL sequence respectively, based on which the spatial SNR (sSNR) and temporal SNR (tSNR) were calculated as described in Shao et al.[22] The *r*MeanB1 and *r*Asym metrices were calculated for each shimming type based on the channel-specific B_1^+ maps, as described in section 2.3. The relative asymmetry of the perfusion signal, noted as perfusion asymmetry, was calculated by manually drawing the masks of the left and right hemispheres, calculating the mean perfusion of both hemispheres, and dividing their absolute difference by their mean. The repeatability of the ASL sequences was evaluated by calculating the intraclass correlation coefficient (ICC) and the average within-subject coefficient of variation (wsCV) of the perfusion signal. To evaluate the performance improvement with pTx B_1^+ shimming, two-way ANOVA was used to compare the rMeanB1, rAsym, and perfusion of pCASL with univ-shim, indv-shim, and CP-shim, with shimming type and subject as the independent variables and visits as repetitions.

The LE of the pCASL sequences was also estimated. Assuming the LE of PASL is 0.95,[11,23] the mean GM cerebral blood flow (CBF) of the central slice was calculated[12,24] (noted as CBF_{PASL}). The mean GM CBF of the pCASL sequences was calculated with LE = 1[12,24] (noted as CBF_{pCASL}), then the estimated LE of the pCASL sequence was CBF_{pCASL}/CBF_{PASL}.

2.5 | Comparison of 3T and 7T pCASL

Five healthy subjects (5 males, age = 27.0 ± 2.6 years, weight = 73.5 ± 9.8 kg, height = 176.0 ± 7.5 cm) were recruited for the comparison of the optimal 7T pCASL and standard 3T pCASL. The pCASL protocol used at 3 T was the benchmark labeling 0 (RF duration = 500 us, RF gap = 420 us, G_{ave} = 0.6 mT/m, and gRatio = 10).[3,17] The pCASL at 7 T was the optimal pCASL (labeling 3), determined by simulation and in vivo evaluation, and CP-shim was used, given its common use for clinical applications. Other imaging parameters included 50 measurements for 5 minutes, TR = 6000 ms, TE = 1.38 ms, labeling duration = 1 second, postlabeling delay = 1.5 seconds, and FA = 10° and 8° for 3 T and 7 T, respectively.[13] The 5 subjects were scanned back-to-back on 3T and 7T scanners with a pseudo-random order. The same preprocessing and perfusion calculation steps were followed as in section 2.4. The mean GM fractional perfusion signal was calculated for each scan and each subject, based on which sSNR and tSNR were calculated. The CBF maps were calculated with a labeling efficiency of 0.85[24] for 3 T and labeling efficiency estimated in section 2.4 for 7 T.

3 | RESULTS

3.1 | Simulation of pCASL parameter optimization

Figure 2 shows the contour map of the simulated LE of RF duration = 300 us (A), 500 us (B), and 800 us (C) with regard to G_{ave} and *gRatio*. The contours are open-ended because the LE calculation was skipped for those parameter sets that violated the hardware slew-rate limit (200 T/m/s). Results of three representative RF durations are shown. The highest weighted-mean LE (weighted average of each B_1^+/B_0 condition) achieved with the three RF durations were 0.81, 0.78, and 0.64, respectively, which showed a decreasing trend of LE with longer RF duration. Indeed, the highest weighted mean LE (0.81) in the whole 3D parameter space (RF duration, G_{ave}, and gRatio) was achieved with RF duration = 300 us, $G_{ave} = 0.3\,\mathrm{mT/m}$, and $gRatio = 11$, which served as labeling 1.

The contour maps of the simulated LE with regard to B_1^+ scaling and B_0 offset are shown in Figure 2D-F for labeling 0, labeling1, and labeling 3, respectively. Compared with labeling 0, labeling 1 and labeling 3 showed greatly reduced variation across the whole B_0 offset frequency range, which suggests increased robustness to B_0 offset, and LE > 0.80 was achieved when B_1^+ scaling factor was larger than 0.6. Compared with labeling 1, the optimal B_1^+ amplitude of labeling 3 was increased from about 70% to about 100% as the result of increased G_{ave},

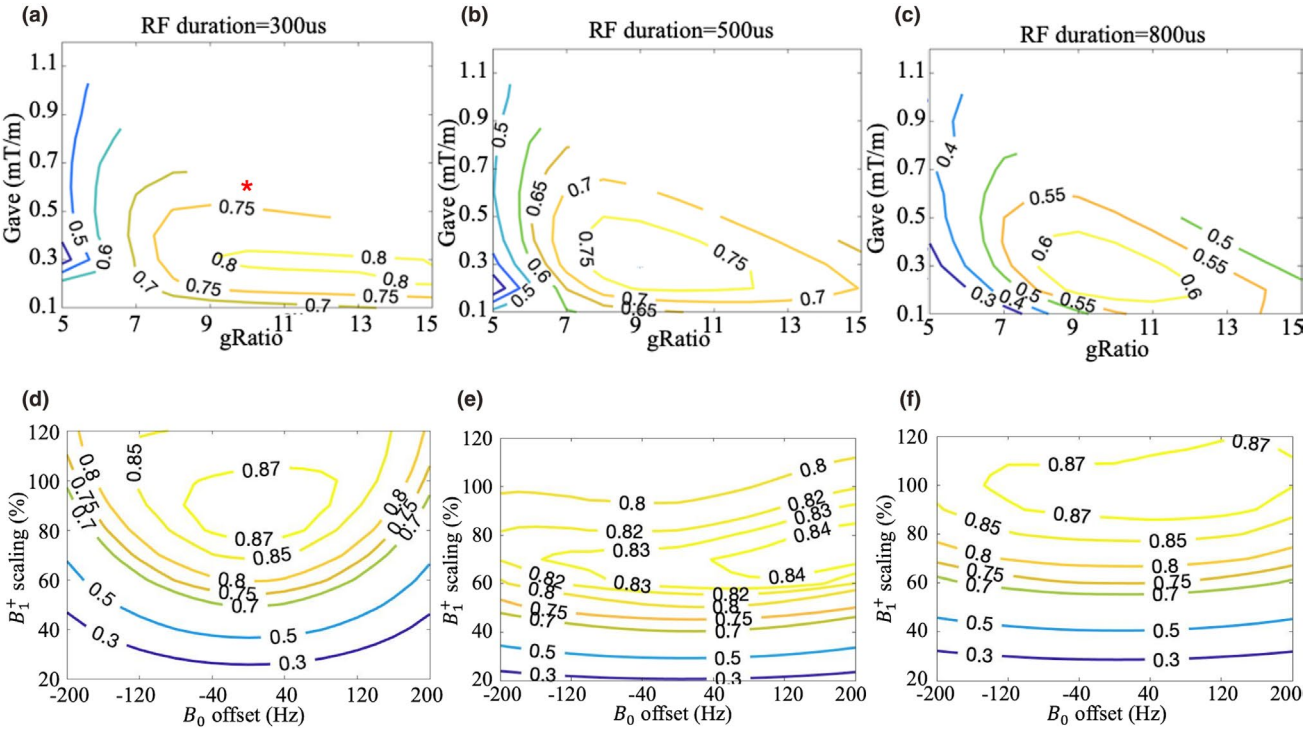

FIGURE 2 A-C, Contour map of the simulated weighted mean labeling efficiency (LE) (weighted average of each B_1^+/B_0 condition) for RF duration = 300 us, 500 us, and 800 us, respectively. The highest weighted-mean LE in the (RF duration, G_{ave}, and *gRatio*) 3D parameter space was achieved with (300 us, 0.3 mT/m, and 11). The red asterisk mark in (A) indicates "labeling 3," which was determined as the final optimal 7T pseudo-continuous arterial spin labeling (pCASL) later. D-F, Simulated LE versus B_1^+ and B_0 for labeling 0, labeling 1, and labeling 3, respectively. Compared with labeling 0 (D), labeling 1 (E) and labeling 3 (F) showed increased robustness to B_0 offset. Compared with labeling 1, labeling 3 showed increased optimal B_1^+ amplitude and lower LE when B_1^+ amplitude was low (< 70%) due to increased G_{ave}

which ameliorated the aliasing of the labeling plane at the cost of lower LE when B_1^+ amplitude was low (< 70%).

3.2 | In vivo evaluation for pCASL parameter optimization

The parameters of the four sets of labeling parameters (labeling 0, 1, 2, and 3) are reported in Table 1. The fractional perfusion map of 1 representative subject is shown in Figure 3, which exhibits perfusion maps possibly contaminated by the side lobes of the pCASL labeling pulses when a smaller gradient was used (labeling 1: $G_{ave} = 0.3\,\mathrm{mT/m}$). This pattern was consistent among the other subjects (Supporting Information Figure S3). Therefore, labeling 1 was dropped from further evaluation. The mean GM fractional perfusion signal was calculated for each labeling parameter set, also reported in Table 1. Labeling 3 had a higher fractional perfusion signal (1.26 ± 0.22%) compared with labeling 0 (1.14 ± 0.26%) and labeling 2 (1.21 ± 0.28%), although without statistical significance due to the limited sample size. Therefore, labeling 3 (red asterisk mark in Figure 2A) was chosen as the optimal 7T pCASL labeling and used later for in vivo experiments.

3.3 | Parallel transmit B_1^+ shimming

3.3.1 | Asymmetry weight evaluation for individual weight

Figure 4 shows the asymmetry weight evaluation process with 2 representative subjects. Figure 4A,D shows the time-of-flight image of the labeling plane as well as the ROI of the inflowing arteries. Figure 4B,E shows the variation of rMeanB1 ratio (indv-shim versus CP-shim) versus the asymmetry weight w, and Figure 4C,F shows the variation of rAsym ratio versus w. Generally, a higher asymmetry weight w led to a lower rMeanB1 ratio and lower rAsym ratio, as the mean B_1 amplitude was sacrificed to achieve lower asymmetry. As a balance between the two terms, $w = 20$ was chosen because it yielded an rAsym ratio < 1 for both subjects while largely preserving mean B_1 amplitude gain from B_1 shimming (rMeanB1 ratio > 1.1). The results of 3 other subjects

TABLE 1 Parameters of the pCASL sequences for the pilot study as well as their perfusion signals

Name	RF duration (us)	RF FA (°)	RF gap (us)	G_{ave}(mT/m)	*gRatio*	Mean perfusion (%)
Labeling 0	500	25	420	0.6	10	1.14 ± 0.26
Labeling 1	300	15	270	0.3	11	0.26 ± 0.08
Labeling 2	300	15	270	0.6	10	1.21 ± 0.28
Labeling 3	300	15	250	0.6	10	1.26 ± 0.22

Note:: Labeling 3 achieved the highest perfusion signal and thus was chosen as the optimal 7T pCASL.

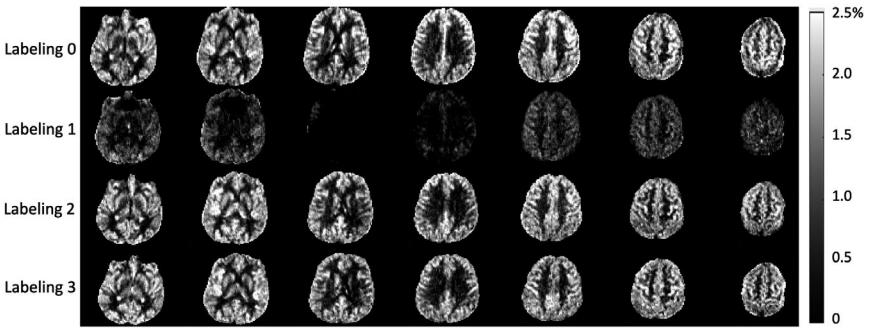

FIGURE 3 Fractional perfusion maps of four pCASL labeling schemes acquired in 1 representative subject. Perfusion map of labeling 1 was clearly contaminated by the labeling side band, whereas the remaining three pCASL perfusion maps were visually similar and evaluated with quantitative analysis

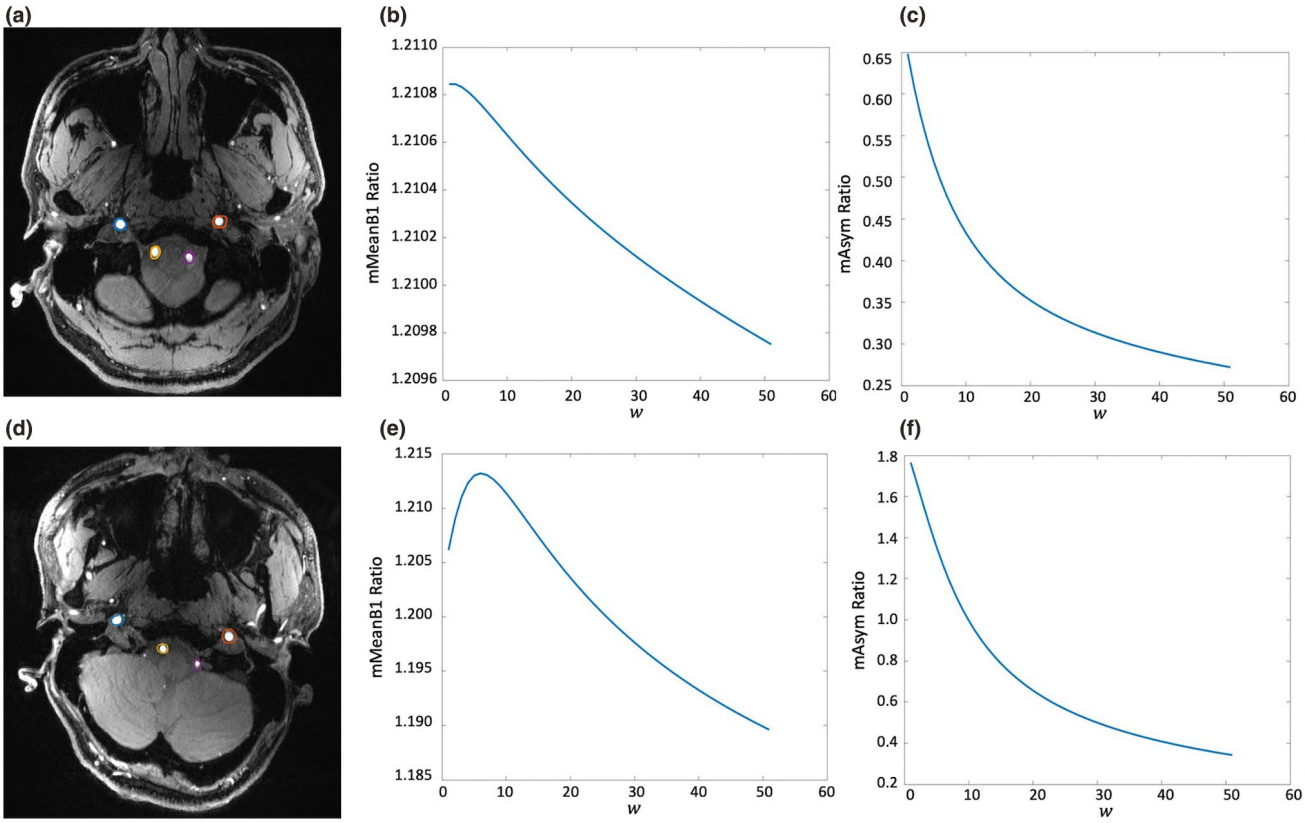

FIGURE 4 A,D, The region-of-interest (ROI) maps on the time-of-flight (TOF) image acquired in 2 subjects. B,E, The rMeanB1 ratio between individual shim (indv-shim) and circularly polarized shim (CP-shim) with w ∈ [0, 50]. C,F, The rAsym ratio with $w \in [0, 50]$. For both subjects, $w = 20$ yielded a consistent increase of rMeanB1 and a smaller rAsym compared with CP-shim

are shown in Supporting Information Figure S4, which validated our choice of $w = 20$.

3.3.2 | Universal weight

The same process as used for indv-shim was performed to determine the optimal asymmetry weight for univ-shim. The rMeanB1 ratio and the rAsym ratio (vs CP-shim) are shown in Figure 5A,B, respectively, and $w = 40$ was chosen with rMeanB1 ratio ≈ 1.14 and rAsym ratio < 1.

The simulated subject-wise rMeanB1 and rAsym for each shimming mode are shown in Figure 5C,D, respectively. With univ-shim, the rMeanB1 was significantly increased compared with CP-shim (0.72 ± 0.06 vs 0.64 ± 0.07; $P < .001$), although lower than the indv-shim (0.75 ± 0.08). In terms of the asymmetry term rAsym, the univ-shim was comparable to the CP-shim (0.13 ± 0.07 and 0.14 ± 0.06, respectively), which were both higher than indv-shim (0.06 ± 0.03). Therefore, the univ-shim was able to increase the mean B_1^+ amplitude by nearly 14%, while maintaining a comparable asymmetry level as the CP-shim in our simulation.

3.4 | In vivo experiment

Calculated with the channel-specific B_1^+ map acquired for two visits of each of the 6 subjects (total 12 measurements), the rMeanB1 and rAsym of three B_1^+ shimming modes are shown in Supporting Information Figure S5A,B. The rMeanB1 was significantly increased with univ-shim compared with CP-shim (0.83 ± 0.10 vs 0.75 ± 0.11; $P < .001$). Although the rMeanB1 of indv-shim was the highest (0.86 ± 0.09), it was not significantly different from that of univ-shim. In terms of rAsym, the univ-shim (0.13 ± 0.06) was slightly lower than the CP-shim (0.14 ± 0.06), with indv-shim being the lowest (0.06 ± 0.03; $P < .01$ against CP-shim and univ-shim, respectively). This result was highly consistent with the simulation results in universal weight evaluation, suggesting that univ-shim was able to increase the mean B_1^+ amplitude within ROIs of inflowing arteries without increasing the asymmetry. Supporting Information Figure S5C shows the amplitude and phase of the combined B_1^+ map of three shimming modes for 1 representative subject. Indv-shim and univ-shim obtained similar combined B_1^+ map. Both indv-shim and univ-shim increased B_1^+ amplitude within the ROIs (colored circles), although at the cost of a dark band (yellow arrow), which would not affect the inflowing arteries.

The fractional perfusion map of 1 representative subject is shown in Figure 6. Perfusion maps of the rest of the 5 subjects are shown in Supporting Information Figure S6. All pCASL sequences achieved perfusion maps of decent quality and good repeatability. The average GM fractional perfusion values of three B_1^+ shimming modes are shown in Figure 7. Compared with perfusion of pCASL with CP-shim ($1.27 \pm 0.13\%$), perfusion of pCASL with indv-shim ($1.39 \pm 0.13\%$) was significantly higher ($P < .05$), which was increased by 9.5%, while perfusion of pCASL with univ-shim ($1.34 \pm 0.14\%$) was 5.3% higher than that of pCASL with CP-shim, although the difference was not significant ($P = 0.35$). In terms of sSNR, pCASL with CP-shim achieved the highest (2.84 ± 0.36), followed by univ-shim (2.83 ± 0.33) and

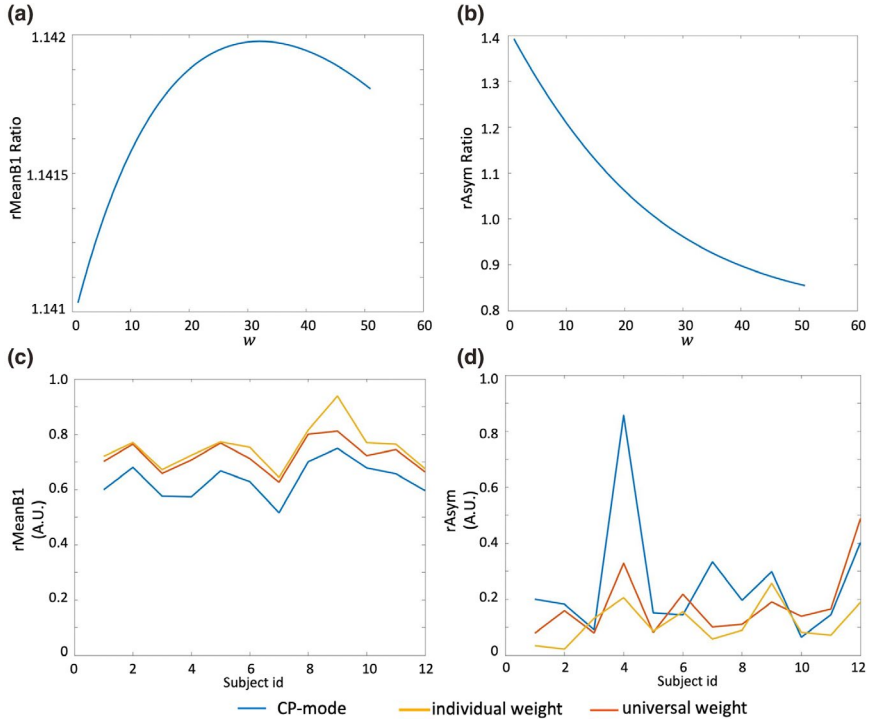

FIGURE 5 A,B, The simulated rMeanB1 ratio and rAsym ratio between universal shim (univ-shim) and CP-shim $w \in [0, 50]$. The value of $w = 40$ was chosen for univ-shim. C,D, The simulated rMeanB1 and rAsym curve of three shimming modes, respectively. The univ-shim achieved considerable mean B_1^+ increase compared with CP-shim for all subjects, which was comparable to indv-shim, although the asymmetry was higher than indv-shim

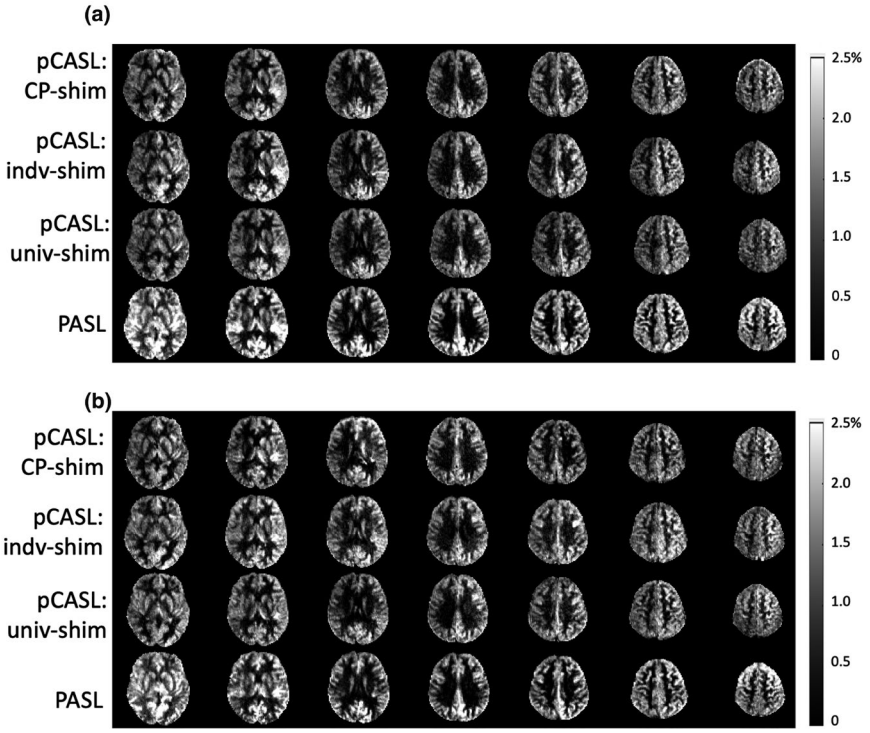

FIGURE 6 Fractional perfusion maps of 1 representative subject: visit 1 (A) and visit 2 (B). Repeatable perfusion maps were obtained with all pCASL sequences, while the difference among the three shimming modes was not observable visually. Abbreviation: PASL, pulsed ASL

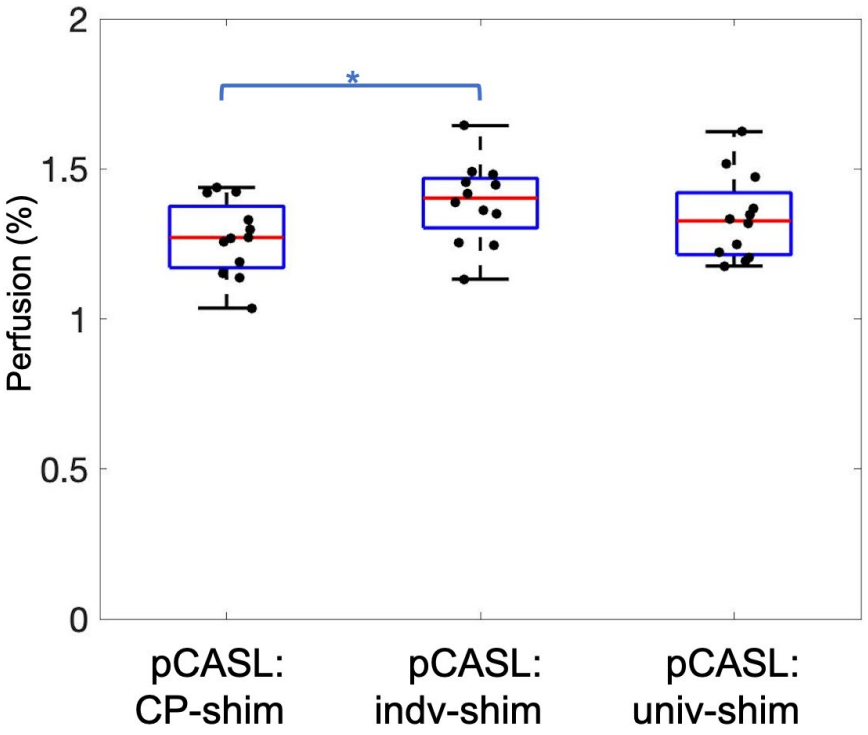

FIGURE 7 Comparison of the mean gray matter (GM) fractional perfusion signals of three shimming modes. Perfusion of pCASL with indv-shim was significantly higher than that of CP-shim (increased by 9.5%; $P < .05$). Perfusion of pCASL with univ-shim was also increased compared with that of CP-shim by 5.3%, although the difference was not significant, probably due to limited sample size

CP-shim (2.79 ± 0.50), although the difference was not significant. The tSNR of pCASL with indv-shim was the highest (1.28 ± 0.14), followed by univ-shim and CP-shim (1.27 ± 0.14 and 1.27 ± 0.16), without statistical significance. The perfusion asymmetry of CP-shim, indv-shim, and univ-shim were 0.090 ± 0.074, 0.087 ± 0.074, and 0.088 ± 0.082, respectively, which was consistent with the rAsym results.

The ICC of pCASL with CP-shim, indv-shim, and univ-shim was 0.66, 0.73, and 0.50, respectively, and the wsCV averaged across subjects was 4.60%, 3.94%, 6.90%, respectively, indicating a good level of repeatability of the three pCASL sequences. The ICC and the average wsCV of the PASL were 0.67 and 7.5%, respectively. The corresponding Bland-Altman plot is shown in Supporting Information Figure S7.

	CP-shim	indv-shim	univ-shim	PASL
rMeanB1	0.75 ± 0.11	0.86 ± 0.09	0.83 ± 0.10	—
rAsym	0.14 ± 0.06	0.06 ± 0.03	0.13 ± 0.06	—
Perfusion (%)	1.27 ± 0.12	1.39 ± 0.13	1.34 ± 0.14	1.35 ± 0.23
sSNR	2.79 ± 0.50	2.84 ± 0.36	2.83 ± 0.33	2.60 ± 0.33
tSNR	1.27 ± 0.16	1.28 ± 0.14	1.27 ± 0.14	1.64 ± 0.29
Perfusion asymmetry	0.090 ± 0.074	0.087 ± 0.074	0.088 ± 0.082	0.070 ± 0.027
ICC	0.66	0.73	0.50	0.67
wsCV (%)	4.60 ± 2.74	3.94 ± 2.68	6.90 ± 4.07	7.51 ± 4.40
LE	0.62 ± 0.10	0.69 ± 0.15	0.66 ± 0.14	0.95

Note:: The pCASL with indv-shim outperforms the other two with the highest rMeanB1 and lowest rAsym, highest perfusion, SNR, intraclass correlation coefficient (ICC), within-subject coefficient of variation (wsCV), and LE. Univ-shim also achieved increased rMeanB1, perfusion, and LE compared with CP-shim.

Abbreviations: sSNR, spatial SNR; tSNR, temporal SNR.

TABLE 2 Quantitative metrics of pCASL sequences with three shimming modes and the PASL sequence

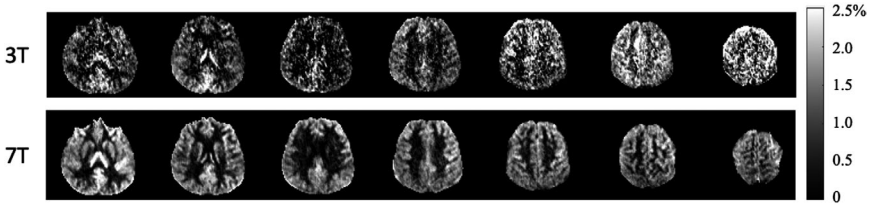

FIGURE 8 Comparison of the fractional perfusion maps of 3T and 7T pCASL. With the same repetition number and scan time, 7T pCASL obtained perfusion maps of superior quality over its 3T counterpart

Assuming the LE of the PASL is 0.95, CBF_{PASL} was calculated to be 58.1 mL/100 g/min, well matching the literature values,[25,26] based on which the LE of pCASL with CP-shim, indv-shim, and univ-shim was estimated to be 0.62, 0.69, and 0.66, respectively. Quantitative indices including rMeanB1, rAsym, perfusion, perfusion asymmetry, SNR, ICC, wsCV, and LE are summarized in Table 2.

3.5 | Comparison of 3T and 7T pCASL

The fractional perfusion maps of 1 representative subject at 3 T and 7 T are shown in Figure 8. The average sSNR of the 3T and 7T pCASL was 1.61 ± 0.47 and 2.87 ± 0.46, respectively, and the average tSNR was 0.39 ± 0.10 and 1.17 ± 0.17, respectively. The optimized 7T pCASL showed superior performance compared with standard 3T pCASL, with a substantial increase of sSNR (by 78.3%) and tSNR (by 200%). Labeling efficiency of 0.62, which was estimated for pCASL with CP-shim, was used to calculate the CBF of 7T pCASL. The mean sSNR, tSNR, and CBF of 3 T and 7 T are reported in Supporting Information Table S2.

4 | DISCUSSION

In this study, we optimized the pCASL parameters based on the distribution of B_1^+/B_0 fields at 7 T and incorporated pTx B_1^+ shimming to further increase the labeling efficiency. The optimized pCASL was able to achieve reliable and repeatable perfusion map with all three B_1^+ shimming modes, and a significantly higher perfusion signal (9.5%) was achieved with indv-shim. In addition, a universal weight for B_1^+ shimming was developed, which does not require any adjustment for individual subjects, and a 5.3% of perfusion signal increase was achieved. Finally, the optimized 7T pCASL was compared with standard 3T pCASL, and the sSNR and tSNR were increased by 78.3% and 200%, respectively.

4.1 | Pseudo-continuous ASL labeling optimization

In this study, the pCASL parameters were optimized specifically for 7T applications (ie, to provide LE with increased robustness to B_0 offset with a lower B_1^+ amplitude). Our simulation yielded labeling 1 (RF duration = 300 us, G_{ave} = 0.3 mT/m, $gRatio$ = 11) as the optimal set of pCASL parameters, which fits with our expectation. Based on the principle of balanced pCASL, the LE has a periodic fluctuation against $\Delta phase$, which is the B_0-induced phase offset between adjacent pulses. Considering that the phase error accrued between adjacent labeling pulses is proportional to (RF [duration+gap]· B_0 offset), a shorter RF duration and gap would improve the robustness to B_0 offset. Meanwhile, according to the flow-driven adiabatic inversion explanation of pCASL,[5] G_{ave} must be reduced accordingly when B_1^+

amplitude is lower; thus, by simulation, 0.3 mT/m (labeling 1) was the optimal G_{ave} instead of the value 0.6 mT/m for labeling 0.[24]

However, a lower G_{ave} and lower gRatio would lead to a thicker labeling plane, which increases the sensitivity of LE to T_2 decay and local B_0 offset. Although B_0 offset estimated from the previous subject cohort (Supporting Information Section 2) was already included in the simulation, variation across subjects can be large, especially with the air–tissue interfaces at the labeling plane, which is challenging to quantify. Subject-wise correction with compensating gradient[27] and protocol optimization with simulation[28] requires extra time and effort. Moreover, the lower G_{ave} of 0.3 mT/m and the shorter RF period would lead to a larger aliasing location of the labeling. As indicated in Supporting Information Section 12 and Figure S8, the aliasing of labeling 1 extended 71 mm away from the labeling plane, which is likely in the imaging volume. Specifically, if the first aliasing is limited to be within 35 mm (as a reference, the typical distance between the bottom edge of the imaging volume and the labeling plane is about 40 mm in this study), the minimum G_{ave} was calculated to be 0.6 mT/m. If this limit was applied in the simulation, the optimal parameter set became RF duration = 300 us, G_{ave} = 0.6 mT/m, and gRatio = 9, which is very close to the current setting. Moreover, a higher duty cycle (the ratio between RF duration and RF period) helps reduce the side lobe amplitude. Considering all of these factors, labeling 3 with the shortest RF duration and gap and a higher G_{ave} and G_{max} was chosen as the optimal pCASL scheme at 7 T, which achieved the highest LE in our study.

It is worth noting that the B_0 offset problem may be addressed with prescans for B_0 offset correction.[14] We simulated LE in the absence of B_0 offset, and the results (see Supporting Information Section 13 and Figure S9) showed that a higher RF duration and a higher gRatio lead to a higher LE without B_0 offset. This may have implications for future 7T pCASL studies adopting prescan B_0 calibrations. The substantial increase of SNR (78.3% of sSNR and 200% of tSNR) achieved with 7T pCASL compared with its 3T counterpart strongly demonstrated the superiority of optimized 7T pCASL over standard 3T pCASL. Note that the image quality of 3T pCASL (Figure 8) was relatively poor compared with previous studies using EPI readout,[22] as we used a higher resolution, TFL readout with small FA, and a reduced labeling duration of 1 second (in comparison to 7 T) in the present study.

4.2 | Parallel transmit B_1^+ shimming

The pTx offers a high degree of freedom to pulse design with the multiple transmit channels driven by their individual RF amplifier. Three main categories of pTx pulse have been proposed previously: the static pTx, in which the same RF waveform is used for all RF channels, and the relative B_1^+ amplitude and phase is adjusted by the channel-specific complex weight; the dynamic pTx, in which each channel is powered with different RF waveforms; and the multipulse pTx, in which the channel-specific weights can change throughout an MRI sequence.

Apparently, the dynamic pTx offers the highest degree of freedom with its channel-specific RF waveform. However, dynamic pTx is challenging for pCASL, given the flowing spins that confound the precise control of the excitation k-space for optimal pTx pulse design.[29] Moreover, the purpose of B_1^+ shimming for pCASL labeling is only to increase B_1^+ amplitude within the inflowing arteries but may lead to possible destructive patterns elsewhere (eg, imaging volume); thus, static pTx is not suitable. Therefore, we chose to use the multipulse pTx in this study, in which the adjusted weight was only used for pCASL labeling, and the CP mode was still used for image acquisition.

Among the pCASL sequences with three shimming modes, pCASL indv-shim achieved the highest LE and ICC at the cost of extra time and effort needed. Inspired by the universal pulse,[16] we proposed univ-shim to improve the workflow of pCASL with pTx B_1^+ shimming. This idea is supported by the observation that despite the cross-subject variation, the location of the inflowing arteries of different subjects is relatively consistent as well as the channel-specific B_1^+ map pattern. Indeed, the universal weight common for different subjects was found, and it was evaluated with cross-validation in simulation and validated in all 6 subjects without any adjustments. We believe this universal weight can be generalized to other sites with the same scanner/RF coil setup, although further validation is needed for a larger cohort of subjects and for subjects with an abnormal distribution of arteries. Therefore, despite its suboptimal performance than the indv-shim, the proposed univ-shim provides a promising solution to the B_1^+ shimming implementation problem for pCASL at 7 T.

For the proposed pCASL B_1^+ shimming, only the phase of the channel-specific weights was optimized, which is only an interim solution for SAR constraint. The best strategy would be to include both global SAR and local SAR constraints into the weight optimization. However, this is not feasible yet due to hardware limitations: theoretically, the local SAR is controlled with a virtual observation point method,[30] which requires the detailed excitation profile information of the RF coil used so that the local SAR hotspots are monitored. However, because that information is not provided by the coil vendor, the local SAR constraint is enforced by limiting the power (or B_1^+ amplitude) of each RF channel very conservatively, leading to higher SAR percentage reading when the B_1^+ shimming mode is turned on, even if the shimming weights are exactly the same as the True-Form mode. When the B_1^+ amplitude varies across channels, the overestimation is even

higher. Therefore, we decided to use the same amplitude for all channel weights and only optimize the phase. Moreover, due to the more constraining SAR limit for univ-shim and indv-shim, the TR was set to 9000 ms compared with 6000 ms for CP-shim, leading to apparently lower SNR efficiency for indv-shim and univ-shim. In the future, once the virtual observation point method is implemented on the scanner, we believe that comparable TR (and thus scan time) can be used for univ-shim and indv-shim as CP-shim, and that more SAR-efficient shimming weights can be obtained with SAR constraints explicitly included in the weight optimization process.

It is worth noting that the VERSE RF modification can be used to ameliorate the SAR constraint problem. However, based on our simulation, VERSE may not be a good fit for pCASL labeling pulse. First, VERSE reduces SAR by stretching/compressing RF waveforms and simultaneously adjusting gradient waveforms. Because the pCASL labeling pulse is very short and the gradient is limited by hardware slew rate, the SAR reduction effect is very limited[31] (eg, only 9.5% SAR reduction with G_{max} increased from 6 mT/m to the "VERSEed" value of 14 mT/m, RF duration = 300 us). Second, a longer gradient ramp time and a longer rewinding gradient of labeling pulses are needed when G_{max} is increased to the "VERSEed" value, leading to a lower RF amplifier duty cycle, which, as demonstrated in Supporting Information Section 12, worsens the aliasing problem. A longer RF duration and RF period could ameliorate the aliasing problem, but the pCASL LE would be more sensitive to B_0 offset. Supporting Information Figure S10 demonstrates the excitation profile (first row) as well as the pulse and gradient waveform (second row) of the optimized pCASL labeling (left column), its VERSE modification (middle column), and VERSE with RF duration = 500 us (right column), respectively. The VERSE modification algorithm was adopted from Gai and Zur.[32]

4.3 | Limitations and future directions

First, the simulation model needs to be expanded to include the pulsatile and laminar flow, an independent RF gap value, and an off-resonance gradient.[27] Second, 2D TFL was used for image acquisition in this study, which could not cover the whole brain during the image acquisition window. More efficient acquisition schemes such as simultaneous multislice[13] and 3D gradient and spin echo can be applied to increase imaging speed and coverage.[33] Third, more SAR-efficiency shimming weights can be obtained by directly including SAR constraint in the optimization and releasing weight amplitude as the subject of optimization once the coil information for the virtual observation point method is available.

5 | CONCLUSIONS

We optimized the pCASL labeling parameters based on the B_1^+/B_0 field distributions at 7 T and further increased the labeling efficiency with pTx B_1^+ shimming of indv-shim and univ-shim. The proposed pCASL methods were able to achieve reliable and repeatable perfusion measurements at 7 T with increased SNR compared to standard 3 T pCASL.

CONFLICT OF INTEREST

Dr. Samantha J. Ma is an employee of Siemens Medical Solutions, USA.

ORCID

Kai Wang https://orcid.org/0000-0003-2752-6953
Samantha J. Ma https://orcid.org/0000-0003-3127-455X
Xingfeng Shao https://orcid.org/0000-0002-4130-6204
Chenyang Zhao https://orcid.org/0000-0002-9841-6332
Qinyang Shou https://orcid.org/0000-0002-3343-3895
Lirong Yan https://orcid.org/0000-0002-5173-7059
Danny J. J. Wang https://orcid.org/0000-0002-0840-7062

REFERENCES

1. Pohmann R, Speck O, Scheffler K. Signal-to-noise ratio and MR tissue parameters in human brain imaging at 3, 7, and 9.4 tesla using current receive coil arrays. *Magn Reson Med*. 2016;75:801-809.
2. Zhang X, Petersen ET, Ghariq E, et al. In vivo blood T1 measurements at 1.5 T, 3 T, and 7 T. *Magn Reson Med*. 2013;70:1082-1086.
3. Wu WC, Fernández-Seara M, Detre JA, Wehrli FW, Wang J. A theoretical and experimental investigation of the tagging efficiency of pseudocontinuous arterial spin labeling. *Magn Reson Med*. 2007;58:1020-1027.
4. Ghariq E, Teeuwisse WM, Webb AG, van Osch MJ. Feasibility of pseudocontinuous arterial spin labeling at 7 T with whole-brain coverage. *MAGMA*. 2012;25:83-93.
5. Dai W, Garcia D, de Bazelaire C, Alsop DC. Continuous flow-driven inversion for arterial spin labeling using pulsed radio frequency and gradient fields. *Magn Reson Med*. 2008;60:1488-1497.
6. Silver M, Joseph R, Hoult D. Highly selective π2 and π pulse generation. *J Magn Reson*. 1969;59:347-351.
7. Kupce E, Freeman R. Adiabatic pulses for wideband inversion and broadband decoupling. *J Magn Reson*. 1995;115:273-276.
8. Ordidge RJ, Wylezinska M, Hugg JW, Butterworth E, Franconi F. Frequency offset corrected inversion (FOCI) pulses for use in localized spectroscopy. *Magn Reson Med*. 1996;36:562-566.
9. Zimmer F, O'Brien K, Bollmann S, Pfeuffer J, Heberlein K, Barth M. Pulsed arterial spin labelling at ultra-high field with a B1(+)-optimised adiabatic labelling pulse. *MAGMA*. 2016;29:463-473.
10. Bause J, Ehses P, Mirkes C, Shajan G, Scheffler K, Pohmann R. Quantitative and functional pulsed arterial spin labeling in the human brain at 9.4 T. *Magn Reson Med*. 2016;75:1054-1063.
11. Wang K, Shao X, Yan L, Ma SJ, Jin J, Wang DJJ. Optimization of adiabatic pulses for pulsed arterial spin labeling at 7 tesla: comparison with pseudo-continuous arterial spin labeling. *Magn Reson Med*. 2021;85:3227-3240.

12. Zuo Z, Wang R, Zhuo Y, Xue R, St Lawrence KS, Wang DJ. Turbo-FLASH based arterial spin labeled perfusion MRI at 7 T. *PLoS One*. 2013;8:e66612.
13. Wang Y, Moeller S, Li X, et al. Simultaneous multi-slice Turbo-FLASH imaging with CAIPIRINHA for whole brain distortion-free pseudo-continuous arterial spin labeling at 3 and 7 T. *Neuroimage*. 2015;113:279-288.
14. Luh WM, Talagala SL, Li TQ, Bandettini PA. Pseudo-continuous arterial spin labeling at 7 T for human brain: estimation and correction for off-resonance effects using a Prescan. *Magn Reson Med*. 2013;69:402-410.
15. Tong Y, Jezzard P, Okell TW, Clarke WT. Improving PCASL at ultra-high field using a VERSE-guided parallel transmission strategy. *Magn Reson Med*. 2020;84:777-786.
16. Gras V, Vignaud A, Amadon A, Le Bihan D, Boulant N. Universal pulses: a new concept for calibration-free parallel transmission. *Magn Reson Med*. 2017;77:635-643.
17. Shao X, Ma SJ, Casey M, D'Orazio L, Ringman JM, Wang DJJ. Mapping water exchange across the blood-brain barrier using 3D diffusion-prepared arterial spin labeled perfusion MRI. *Magn Reson Med*. 2019;81:3065-3079.
18. Zhao L, Vidorreta M, Soman S, Detre JA, Alsop DC. Improving the robustness of pseudo-continuous arterial spin labeling to off-resonance and pulsatile flow velocity. *Magn Reson Med*. 2017;78:1342-1351.
19. Krishnamurthy LC, Liu P, Xu F, Uh J, Dimitrov I, Lu H. Dependence of blood T2 on oxygenation at 7 T: in vitro calibration and in vivo application. *Magn Reson Med*. 2014;71:2035-2042.
20. Maccotta L, Detre JA, Alsop DC. The efficiency of adiabatic inversion for perfusion imaging by arterial spin labeling. *NMR Biomed*. 1997;10:216-221.
21. Nistler J, Diehl J, Renz W, Eberler L. Homogeneity improvement using a 2 port birdcage coil. In Proceedings of the 15th Annual Meeting of ISMRM, Berlin, Germany, 2007. Abstract 1063.
22. Shao X, Wang Y, Moeller S, Wang DJJ. A constrained slice-dependent background suppression scheme for simultaneous multislice pseudo-continuous arterial spin labeling. *Magn Reson Med*. 2018;79:394-400.
23. Wong EC. Quantifying CBF with pulsed ASL: technical and pulse sequence factors. *J Magn Reson Imaging*. 2005;22:727-731.
24. Alsop DC, Detre JA, Golay X, et al. Recommended implementation of arterial spin-labeled perfusion MRI for clinical applications: a consensus of the ISMRM perfusion study group and the European consortium for ASL in dementia. *Magn Reson Med*. 2015;73:102-116.
25. Parkes LM, Rashid W, Chard DT, Tofts PS. Normal cerebral perfusion measurements using arterial spin labeling: reproducibility, stability, and age and gender effects. *Magn Reson Med*. 2004;51:736-743.
26. Pantano P, Baron JC, Lebrun-Grandié P, Duquesnoy N, Bousser MG, Comar D. Regional cerebral blood flow and oxygen consumption in human aging. *Stroke*. 1984;15:635-641.
27. Jahanian H, Noll DC, Hernandez-Garcia L. B0 field inhomogeneity considerations in pseudo-continuous arterial spin labeling (pCASL): effects on tagging efficiency and correction strategy. *NMR Biomed*. 2011;24:1202-1209.
28. Lorenz K, Mildner T, Schlumm T, Möller HE. Characterization of pseudo-continuous arterial spin labeling: simulations and experimental validation. *Magn Reson Med*. 2018;79:1638-1649.
29. Katscher U, Börnert P, Leussler C, van den Brink JS. Transmit SENSE. *Magn Reson Med*. 2003;49:144-150.
30. Eichfelder G, Gebhardt M. Local specific absorption rate control for parallel transmission by virtual observation points. *Magn Reson Med*. 2011;66:1468-1476.
31. Teeuwisse WM, Webb AG, van Osch MJ. Arterial spin labeling at ultra-high field: all that glitters is not gold. *Int J Imaging Syst Technol*. 2010;20:62-70.
32. Gai ND, Zur Y. Design and optimization for variable rate selective excitation using an analytic RF scaling function. *J Magn Reson*. 2007;189:78-89.
33. Spann SM, Shao X, Wang DJ, et al. Robust single-shot acquisition of high resolution whole brain ASL images by combining time-dependent 2D CAPIRINHA sampling with spatio-temporal TGV reconstruction. *Neuroimage*. 2020;206:116337.

SUPPORTING INFORMATION

Additional supporting information may be found online in the Supporting Information section.

FIGURE S1 The labeling block can be described precisely by the timing parameters of RF duration and RF gap, and the gradient parameters G_{max} and G_{ave}. The value of G_{max} can be replaced by $gRatio$: $G_{max} = G_{ave} \cdot gRatio$

FIGURE S2 Flow chart of parallel transmit (pTx) B_1^+ shimming

FIGURE S3 Perfusion maps of the remaining 3 subjects with labeling 1. Severe contamination by the pseudo-continuous arterial spin labeling (pCASL) side band was observed in the imaging volume. The seemingly different location of the side band was due to the different labeling offset, which was adjusted for each subject

FIGURE S4 The region of interest (ROI) maps (left), rMeanB1 ratio versus *w* curve (middle), and rAsym ratio versus *w* curve (right). For all subjects, $w = 20$ yielded a consistent increase of mMeanB1 and a comparable if not smaller mAsym compared with circularly polarized (CP) shim (CP-shim)

FIGURE S5 The rMeanB1 (A) and rAsym (B) curves of the three shimming modes measured from two visits of the 6 subjects (total of 12 measurements) of an in vivo experiment. Individual shim (indv-shim) had consistently higher rMeanB1 than CP-shim for each subject, and universal shim (univ-shim) had similar performance as indv-shim except for measurement 9. The indv-shim had the lowest rAsym, whereas the rAsym of CP-shim and univ-shim were comparable. C, The combined B_1^+ map of 1 representative subject for the three shimming modes (first row, amplitude; second row, phase). Performance of indv-shim and univ-shim were comparable, both of which achieved higher B_1^+ amplitude within ROI (colored circles) compared with CP-shim. A dark band appeared (yellow arrow) with indv-shim and univ-shim, which would not affect the inflowing arteries

FIGURE S6 A-E, The fractional perfusion map for the remaining 5 subjects, respectively (top panel, first visit; bottom panel, second visit). Perfusion maps of good quality and decent repeatability were achieved with all pCASL sequences

FIGURE S7 Bland-Altman plot of pCASL with CP-shim (A), indv-shim (B), and univ-shim (C), and the pulsed ASL

(PASL) sequence (D). All ASL sequences showed decent repeatability

FIGURE S8 The excitation profile of labeling 0, 1, 2, and 3 on the static tissue

FIGURE S9 Contour map of the simulated labeling efficiency (LE) of RF duration = 300 us, 500 us, and 800 us, respectively, with B_0 offset = 0. The same layout was used as in Figure 2A-C. Without B_0 offset, a higher RF duration and a higher gRatio lead to higher LE. The highest LE achieved was 0.874, which was achieved with RF duration = 1000 us, gRatio = 15, and Gave = 0.3 mT/m

FIGURE S10 Excitation profile, RF, and gradient waveform of the optimized pCASL labeling (left column), variable-rate selective excitation (VERSE)–modified pCASL labeling (middle column), and VERSE modified with RF duration = 500 us (right column). The highest gradient during VERSE pulse is 14 mT/m, and the slew rate is 200 mT/m/s. Without VERSE modification, the labeling block parameters are RF duration = 300us, $G_{max.}$ = 6mT/m, gradient ramp time = 30 us, duration of the rewinding gradient = 190 us, RF period = 550 us, and RF duty cycle = 300/550 = 54.6%. With VERSE modification, RF duration = 300 us, gradient ramp time = 70 us, duration of the rewinding gradient = 220 us, RF period = 660 us, and RF duty cycle = 300/660 = 45.6%. Clear aliasing pattern was observed in (B). As observed in (C), when the modified RF duration was increased to 500 us, the aliasing pattern disappeared

TABLE S1 Scan protocol for the in vivo experiments. Note: *TR = 6000 ms for pCASL with CP-shim, and 9000 ms for pCASL with univ-shim and indv-shim, due to more constraining specific absorption rate (SAR) limits (see section 4.2).

TABLE S2 The SNR and cerebral blood flow of 3T and 7T pCASL. Note: The 7T pCASL showed substantially increased SNR (both spatial SNR and temporal SNR) compared with 3T pCASL. Discrepancy between the cerebral blood flow (CBF) values may originate from the inaccuracy estimation of 3T pCASL due to small number of measurements.

How to cite this article: Wang K, Ma SJ, Shao X, et al. Optimization of pseudo-continuous arterial spin labeling at 7T with parallel transmission B1 shimming. *Magn Reson Med*. 2022;87:249–262. https://doi.org/10.1002/mrm.28988